

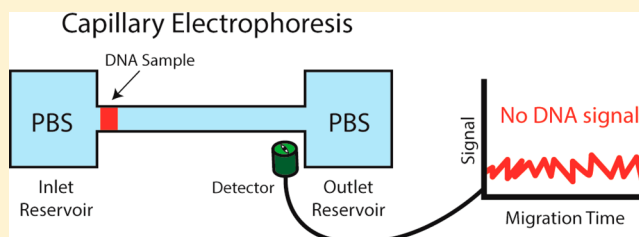
# Analysis of DNA in Phosphate Buffered Saline Using Kinetic Capillary Electrophoresis

Mirzo Kanoatov and Sergey N. Krylov\*

Department of Chemistry and Centre for Research on Biomolecular Interactions, York University, Toronto, Ontario M3J 1P3, Canada

## Supporting Information

**ABSTRACT:** Kinetic capillary electrophoresis (KCE) methods are useful in the study of kinetics and equilibrium properties of interactions between DNA and its binding partners (ligands). KCE experiments are typically performed in a narrow set of “conventional” low-conductivity run buffers while DNA–ligand interactions in biological systems occur in physiological fluids, characterized by high ionic strengths. The nature and ionic strength of the buffer, in which DNA–ligand interaction occurs, can significantly influence the binding. Therefore, KCE experiments meant to study such interactions would greatly benefit if they could be performed in physiological buffers, such as phosphate buffered saline (PBS). No previous KCE studies of DNA used PBS as the run buffer. Here, we test the feasibility of using PBS as a KCE run buffer for analysis of DNA and show that its usage under standard KCE conditions renders DNA undetectable. We uncover the causes of this previously unreported detrimental effect and come up with a modification of KCE which allows one to overcome it. We apply the modified KCE method to an experimental model of a platelet-derived growth factor (PDGF) protein and its DNA aptamer, which was selected in PBS, and show that the results obtained in PBS run buffer are much closer to previously reported values than those which were obtained with a conventional low-conductivity capillary electrophoresis (CE) buffer.



Beyond its vital biological role of encoding genetic information, DNA possesses a number of physical and chemical properties which make it important in bioengineering applications. The large diversity of three-dimensional structures that DNA chains can assume and the availability of relatively simple methods to synthesize, amplify, ligate, and assemble its strands have enabled DNA molecules to be used as probes for affinity interactions,<sup>1</sup> as scaffolds for nanostructure assemblies,<sup>2</sup> and even as building blocks for nanoscale machines.<sup>3,4</sup> Due to the remarkable charge density and easily predictable charge-to-size ratio of its chains, electrophoresis-based methods have been especially useful in analysis and manipulation of DNA.<sup>5</sup> In particular, capillary electrophoresis (CE) methods have been instrumental in such applications as DNA sequencing,<sup>6</sup> hybridization assays,<sup>7,8</sup> and postsynthesis and amplification purity control.<sup>9</sup> Furthermore, in the past two decades, kinetic capillary electrophoresis (KCE) methods have become an attractive means to study the kinetics and thermodynamics of interactions between DNA and their binding partners (ligands),<sup>10,11</sup> as well as for highly efficient selection of DNA aptamers.<sup>12</sup> Benefits of KCE for these applications include unmatched resolving efficiency, superb accuracy and precision of measurements, low sample consumption, and compatibility with sensitive detection methods, such as laser-induced fluorescence (LIF).<sup>13</sup>

Like all electrophoresis-based methods, KCE is limited in the type of run buffers with which it is compatible. A review of recent literature has revealed that the vast majority of KCE

experiments, either aimed at analysis of DNA or other types of molecules, are performed using a narrow set of low ionic strength and low ionic mobility run buffers, with Tris and tetraborate solutions of 20–50 mM ionic strength being the most common.<sup>14–24</sup> Preference for these buffers is often justified by their relatively small degree of Joule heating and slow time of ion depletion. The restricted variety of compatible run buffers, however, is a major drawback of KCE, as in some cases it may weaken the relevance of produced analytical data to the corresponding processes in cells. Affinity interactions are sensitive to their environment and may be altered by such factors as the ionic strength of the solution, its pH, temperature, and the presence of cofactors and stabilizing agents. Thus, for KCE measurements to be meaningful, affinity experiments must be performed in environments that enable the studied molecules to assume their natural, or intended, conformation. As DNA aptamers are often created for use as *in vivo* imaging probes, drug delivery vectors, and even drugs themselves,<sup>25</sup> selection and analysis of such DNA aptamers must be performed in physiological conditions, e.g., in phosphate buffered saline (PBS), the most commonly used physiological buffer in biology and medicine. Our own experience shows (as it will be exemplified in this Article) that results of KCE

Received: May 30, 2016

Accepted: June 24, 2016

Published: June 24, 2016



measurements performed in nonphysiological buffers often diverge from values obtained by alternative methods in PBS. Thus, KCE methods would benefit greatly if they could be performed with PBS as the run buffer. Despite the obvious benefits of such applications, PBS has been used as a CE run buffer only a few times.<sup>26–29</sup> More surprisingly, we did not find any reports where PBS was used as a CE run buffer for analysis of DNA samples.

In this Article, we test the suitability of PBS as a KCE run buffer for analysis of DNA–ligand binding and show that its use under standard KCE conditions renders DNA undetectable. We show that this previously unreported detrimental effect is caused by a combination of phenomena which include: (i) rapid buffer depletion, (ii) unstable electroosmotic flow (EOF), (iii) severe peak broadening, and (iv) extremely low mobility of DNA. After unravelling the causes for this compounded effect, we suggest an approach to overcome the DNA detection problem in PBS by employing a pressure-assisted modification of KCE. We demonstrate the feasibility of this approach by using an experimental model of platelet-derived growth factor (PDGF) protein and its DNA aptamer. We show that the results obtained in PBS run buffer (PBS-KCE) are much closer to previously reported values than the results obtained with a conventional CE buffer (CB)-KCE. This approach significantly improves the analytical value of KCE methods by making the results more relevant to *in vivo* applications. We hope that our documentation of this problem, as well as one of its solutions, will help overcome similar issues in other electrophoresis-based platforms.

## MATERIALS AND METHODS

All chemicals and buffer components were purchased from Sigma-Aldrich (Oakville, ON, Canada) unless otherwise stated. Human PDGF-BB recombinant protein was purchased from R&D Systems (MN, USA). Fused-silica capillaries were purchased from Molex (AZ, USA). DNA aptamer (36t) with affinity toward PDGF protein was selected previously by others<sup>30</sup> and was custom synthesized by Integrated DNA Technologies (Coralville, IA). The nucleotide sequence of the Alexa Fluor 488-labeled, single-stranded DNA aptamer was: 5′-/Alexa 488/-CAC AGG CTA CGG CAC GTA GAG CAT CAC CAT GAT CCT GTG-3′. NanoDrop-1000 spectrometer (Thermo Scientific, Wilmington, DE) was used to verify DNA concentration in the stock solution by measuring light absorbance at 260 nm and dividing the absorbance by a manufacturer-provided extinction coefficient. Concentration of the PDGF-BB protein was measured using a Bicinchnonic acid assay kit from ThermoFisher Scientific (Waltham, MA) according to manufacturer's instructions and using the same spectrophotometer.

**Capillary Electrophoresis.** All CE experiments were carried out using P/ACE MDQ instrument (Beckman Coulter, Mississauga, ON), equipped with a standard fluorescence detector and a 488 nm line of continuous Wave Solid-State laser (JDSU, Santa Rosa, CA) for fluorescence excitation. Runs were performed in uncoated fused-silica capillaries with inner diameters of 75  $\mu\text{m}$  and outer diameters of 360  $\mu\text{m}$ . Capillaries of total lengths of 30 or 50 cm were used as denoted. In both cases, the detection window was 10.1 cm away from the outlet end of the capillary. Times of pressure application which yielded desired volumes of hydrodynamic injection were calculated using CE Expert software, version 2.2 from Sciex (Concord, ON), for each given total length of the capillary.

Two electrophoresis run buffers were compared in these experiments: conventional CE buffer (CB): 50 mM Tris-HCl, pH 7.4; PBS: 8.1 mM  $\text{Na}_2\text{HPO}_4$ , 1.5 mM  $\text{KH}_2\text{PO}_4$ , 137 mM NaCl, 2.7 mM KCl, pH 7.4. Both the inlet and the outlet reservoirs always contained the electrophoresis run buffer of choice. Prior to every run, the capillary was rinsed with the run buffer at 20.0 psi (138 kPa) for a time sufficient to pump 10 capillary volumes. At the end of each run, the capillary was rinsed with a succession of 100 mM HCl, 100 mM NaOH, and deionized water, at the same pressure/time settings. The samples were injected into the capillary, which was prefilled with the run buffer, by a 0.50 psi (3.4 kPa) pressure to yield a 5 mm long sample plug.

**Nonequilibrium Capillary Electrophoresis of Equilibrium Mixtures.** Nonequilibrium capillary electrophoresis of equilibrium mixtures (NECEEM) experiments were performed to study the interaction between PDGF protein and its DNA aptamer. Total capillary length in NECEEM experiments was 50 cm. Plugs of equilibrium sample mixtures were injected from the inlet end of the capillary, and electrophoresis was carried out with the positive electrode at the injection end (inlet end). The sample mixture was propagated through the uncooled portion of the capillary by injecting a 4 cm long plug of running buffer with a 0.50 psi (3.4 kPa) pressure at zero voltage.<sup>31</sup> Dilutions of all sample components were prepared with the electrophoresis run buffer, to minimize issues from electrolyte mismatch between the sample plug and the run buffer. Sample mixtures were incubated at room temperature for 15 min prior to injection to achieve equilibration in the binding reaction. To ensure the best accuracy of the measured  $K_d$  values, the concentrations of equilibrium mixture components were adjusted on the basis of  $K_d$  values obtained from preliminary experiments. The presented NECEEM experiments were performed with protein concentrations similar to preliminary  $K_d$ , while the concentration of the aptamer was lower than the preliminary  $K_d$ . For the CB experiments, the final concentrations of equilibrium mixture components were: 100 nM PDGF, 40 nM aptamer, and 100 nM BODIPY (internal standard and EOF marker). Electrophoresis was carried at a 500 V/cm electric field. The capillary coolant temperature was set to 21 °C. The internal capillary temperature of 25 °C (in the cooled region) was calculated using the simplified universal method for determining electrolyte temperatures (SUMET) based on the readings of electrical current from the CE instrument.<sup>32,33</sup> For PBS experiments, the final concentrations of equilibrium mixture components were: 5 nM PDGF, 1 nM aptamer, and 2.5 nM BODIPY. In addition, 1 mg/mL of BSA protein was added to the equilibrium mixture to prevent adsorption of DNA onto the plastic sample vial. Electrophoresis was carried at a 200 V/cm electric field. The capillary coolant temperature was set to 22 °C, with internal capillary temperature calculated to be 25 °C. Further, for PBS-NECEEM experiments, a pressure of 0.30 psi (2.1 kPa) was applied from the inlet end of the capillary to supplement the electric field. Each experimental point was measured in triplicates, with a fresh equilibrium mixture prepared for each replicate. Electropherograms were analyzed using previously described area deconvolution software (NAAP).<sup>15</sup>

**Mobility Measurements.** To estimate the mobility of DNA with the standard KCE procedure, a sample mixture of 1  $\mu\text{M}$  BODIPY (mobility marker), 100 nM fluorescein (mobility marker), 100 nM DNA aptamer, and 1 mg/mL BSA was used. Electrophoresis was performed in both buffers using the same

conditions as in the NECEEM experiments, except that, in the PBS experiments, no pressure was coapplied with the electric field.

To estimate the mobility of DNA in a capillary with a shortened effective length, the postinjection pressure propagation step was modified to increase the pressure–propagation distance to 9 cm. A 30 cm (total length) capillary was used for these experiments, with a sample being injected from the outlet end of the capillary. This reduced the distance between the initial sample position and the detection window to 1.1 cm. The electric field was applied with the positive electrode at the injection end (outlet). Due to the poor separation in the very short effective length of the capillary, fluorescein was excluded from the sample mixture to avoid its convolution with the BODIPY peak.

To estimate the stability of EOF over time, a 30 cm (total length) capillary was used, with sample injected from the outlet end of the capillary, and the electric field was applied with the positive electrode at the same end. Plugs of 100 nM BODIPY were injected into the capillary with intervals of 260 s, and electrophoresis was carried out without run buffer replenishment between the injections. No pressure propagation of the sample was applied after each sample injection. Signal was only recorded during electrophoresis and not during vial changeover and sample injection. After all of the electrophoresis steps, a small volume of the buffer from electrophoresis reservoirs was deposited onto Alkacid Test Ribbon (ThermoFisher Scientific, Waltham, MA) to approximate the pH of the solution.

## RESULTS AND DISCUSSION

**Undetectable DNA.** To illustrate how the choice of a run buffer can influence KCE results, we performed nonequilibrium capillary electrophoresis of equilibrium mixtures (NECEEM) experiments with a binding pair of PDGF protein and its DNA aptamer. The aptamer for PDGF protein was selected in PBS. As a point of reference, the  $K_d$  of the interaction measured in PBS using nitrocellulose binding assay was reported as 96 pM.<sup>30</sup> We first performed NECEEM with a conventional CE run buffer (CB), 50 mM Tris-HCl, which has the same pH of 7.4 as PBS but a 3-time lower ionic strength. In-capillary temperature was calculated to be 25 °C. The  $K_d$  value, which resulted from these CB-NECEEM experiments, was 56 nM, almost 3 orders of magnitude higher than the value reported in the original publication on the PDGF–aptamer interaction (Figure 1A).

To test if this buffer difference could be responsible for such a drastic discrepancy in measured  $K_d$  or if it arises from more inherent differences in the methodologies, we set out to perform NECEEM experiments with PBS as the run buffer. On the basis of the available recommendations from the literature, we expected that the main difficulty in using PBS will lie in excessive Joule heating due to its high ionic strength and high mobility of its ions, compared to conventional CE buffers. This issue was relatively simple to handle, as convenient in-capillary temperature determination methods, i.e., SUMET,<sup>32,33</sup> allowed us to select the strength of the applied electric field which results in a desired temperature. Thus, for our PBS-NECEEM experiments, we decreased the applied electric field to yield the same 25 °C in-capillary temperature as in CB-NECEEM. The results of the experiment were quite unexpected. As seen in Figure 2, the two migration markers, which were included in the sample mixture, had traveled to the detector with velocities only twice slower than in CB-NECEEM; the signal for the

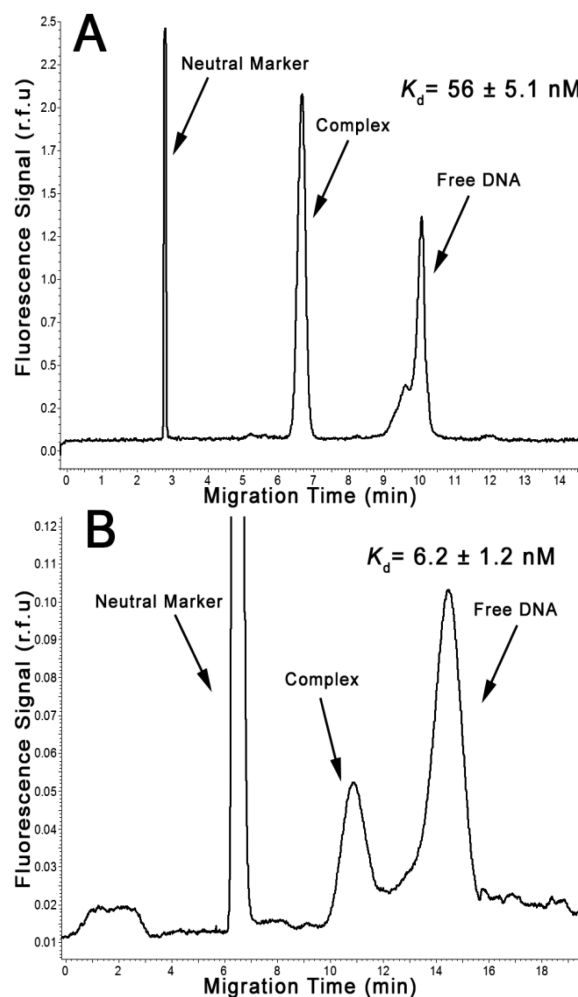


**Figure 1.** Comparison of NECEEM analysis performed in CB (panel A) and PBS (panel B). Sample in the CB experiment contained 100 nM BODIPY, 100 nM PDGF, and 40 nM aptamer. Sample in the PBS experiment contained 2.5 nM BODIPY, 5 nM PDGF, and 1 nM aptamer. Experiment in PBS was performed with the pressure-assisted modification of KCE. The added pressure was 0.30 psi (2.1 kPa). The  $K_d$  value measured in PBS is significantly closer to the value measured by the nitrocellulose membrane-binding assay.

fluorescently labeled DNA, however, did not appear even after 3 h of electrophoresis. The same was true in both the presence and absence of the protein target and for experiments performed with electrode polarities in both positive-to-negative and negative-to-positive arrangements. These results reveal a potential reason as to why the use of PBS as a CE run buffer for analysis of DNA had not been previously documented, despite the attractiveness of such an application. It had become apparent that to facilitate PBS-KCE experiments a better understanding of phenomena underlying the DNA detectability problem is required.

Possible reasons for analyte-specific lack of detectability in CE-LIF can be reduced to three basic causes: (i) reduced detectability of the fluorophore label in a given environment; (ii) insufficient duration of the experiment for the analyte to reach the detector; or (iii) severe smearing of an analyte over the length of the capillary. To eliminate the observed artifact, we need to understand which of these possible causes contribute to the lack of DNA detectability.



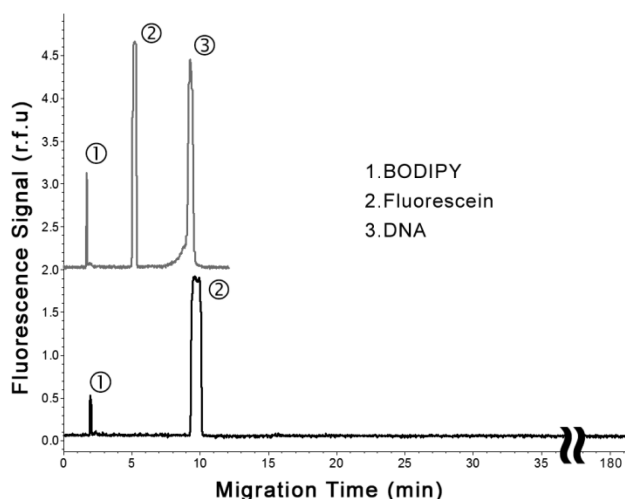


**Figure 2.** Lack of DNA detectability in PBS-KCE. A sample mixture of 1  $\mu\text{M}$  BODIPY, 100 nM fluorescein, and 100 nM of fluorescently labeled DNA aptamer was analyzed by CE with two different running buffers: CB (top trace) and PBS (bottom trace). In PBS, while both migration markers, BODIPY (neutral) and fluorescein (negative), are detected, DNA is not detected even after 3 h of analysis. The PDGF target was not included in these experiments. Migration times of BODIPY reflect velocity of the electroosmotic flow.

**Fluorescence Intensity.** The most discernible reason for lack of sample detectability in LIF is poor intensity of fluorescence. Intensity of a fluorophore strongly depends on its environment,<sup>34</sup> and the fluorescent label on our DNA molecules may have a diminished capacity to absorb or emit photons in the PBS buffer. To decouple the effects associated with fluorescence intensity from the effects associated with electrophoretic migration, we tested if the fluorescently labeled DNA can be detected with pressure-driven propagation through the capillary. As the presence of PDGF did not influence the outcome of our previous runs, we simplified the sample mixture by excluding the protein from all of the subsequent experiments, unless otherwise stated. As shown in Figure S1A, fluorescence from labeled DNA was observed with pressure driven propagation, albeit with poor signal repeatability. We had previously reported on this repeatability issue in DNA analysis which is caused by the interaction of DNA with the walls of the vial used for sample mixture preparation.<sup>35</sup> Interestingly, this behavior seems to be more prominent in PBS than in CB, suggesting that the additional ions in PBS facilitate the interaction of DNA with the plastic walls. To minimize this behavior, we have added 1 mg/mL of bovine serum albumin (BSA) to the sample mixture to passivate the surface of the vial, which has dramatically improved the repeatability of signal intensity (Figure S1B). It should be noted that using BSA as a surface passivating agent may not be suitable for all applications, and users are encouraged to consider some of the many available alternatives depending on the specifics of the experiment.<sup>35</sup> These experiments show that the fluorescence of Alexa Fluor 488-labeled DNA is not suppressed in PBS. This is not a surprising finding, as Alexa Fluor 488 is known to be resilient to environmental changes and is routinely used in PBS.<sup>36,37</sup> To test if the DNA–vial interaction was responsible for the lack of DNA detectability in PBS-NECEEM, we have performed electrophoresis with the BSA-containing sample but still failed to observe the DNA peak. This suggests that electrophoresis plays a central role in the DNA

detectability problem. To avoid the signal repeatability issue due to adsorption of DNA to the vial walls, all subsequent experiments were carried out with 1 mg/mL BSA added to the sample mixture.

**Analyte Velocity.** In CE, an analyte may not be detected if an insufficient amount of time had been allotted for it to reach the detector. Even though our previous PBS-NECEEM experiments had lasted for 3 h, an excessive time for a typical CE run, it might not be sufficient if the analyte velocity is less than 1 mm min<sup>-1</sup>. To directly measure a low velocity in a manageable time frame, we needed to perform electrophoresis in a shorter length of capillary. While the employed commercial CE instrument allows a minimum of 10 cm capillary length to detector, the effective distance of migration can be shortened further by pressure-propagating the sample closer to the detector before electric field application. By employing this technique, we performed electrophoresis with the sample plug starting position being 1.1 cm away from the detector. Shortening the electrophoresis distance had allowed us to observe the DNA peak in PBS-KCE (Figure 3), which migrated

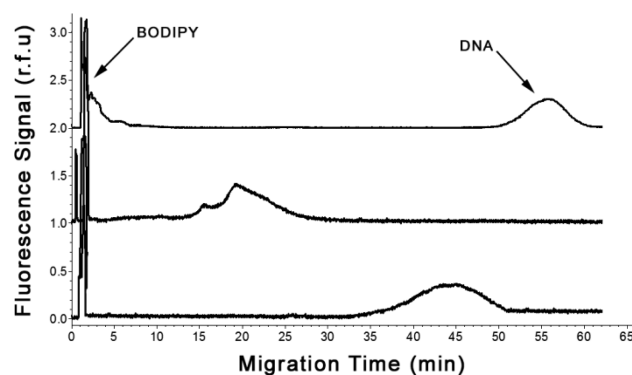


**Figure 3.** Mobility of DNA in PBS-KCE experiment, performed in 11 mm effective capillary length. A plug of 1  $\mu\text{M}$  BODIPY and 100 nM fluorescently labeled DNA aptamer was injected into a 10.1 cm to detector capillary and was propagated 9 cm by pressure. The three stacked traces show trials of the same experiment in chronological order (first experiment at the bottom, last at the top). DNA migration velocity has very poor repeatability.

with low velocities in a range of 0.2–0.6 mm min<sup>-1</sup>. At this range of velocities, it would take over 20 h for DNA to traverse the standard capillary length to detector of 40 cm. To understand what causes the DNA to slow down to a near-stationary migration in PBS-KCE, we need to take into account the different mobility vectors that define it. Velocity of an analyte in CE is determined by its total mobility ( $\mu_{\text{tot}}$ ) and the strength of the applied electric field. The above measurement shows that  $\mu_{\text{tot}}$  of DNA is  $\sim 0.003 \text{ mm}^2 \text{ V}^{-1} \text{ min}^{-1}$ . In bare-silica capillaries,  $\mu_{\text{tot}}$  of DNA is a sum of two opposing vectors: mobility of the EOF ( $\mu_{\text{EOF}}$ ), directed toward the cathode, and the electrophoretic mobility of DNA ( $\mu_{\text{eph}}$ ), directed toward the anode. EOF is a bulk flow, meaning that its mobility vector affects all analytes equally. The magnitude of  $\mu_{\text{EOF}}$  is inversely proportional to the ionic strength of the solution, and since the ionic strength of PBS is greater, its  $\mu_{\text{EOF}}$  is lower than in CB, 2.25 and 3.85 mm<sup>2</sup> V<sup>-1</sup> min<sup>-1</sup>, respectively (Figure 2). The near-stationary  $\mu_{\text{tot}}$  of DNA, thus, can arise if the magnitude of  $\mu_{\text{eph}}$  is similar to the magnitude of  $\mu_{\text{EOF}}$ . Interestingly, the  $\mu_{\text{eph}}$  of DNA in CB-NECEEM is  $-2.20 \text{ mm}^2 \text{ V}^{-1} \text{ min}^{-1}$  (negative sign signifies that it opposes the flow of the electrical current),

suggesting that it does not change significantly upon transition from CB to PBS.

Besides revealing the small magnitude of DNA  $\mu_{\text{tot}}$ , results in Figure 3 also reveal two additional complications: first, the migration of DNA in PBS-NECEEM has very poor repeatability, with elution times ranging between 20 and 60 min; second, the peaks manifested significant broadening and loss of intensity. It is possible that the poor repeatability of DNA migration time, observed in Figure 3, was caused by imprecisions in the pressure propagation step, introduced to shorten the effective capillary length; however, a similar experiment performed with CB demonstrates that sample propagation by itself does not cause migration repeatability issues (Figure S2), establishing the fact that these effects are tied to electrophoresis in PBS. Many (if not most) migration non-repeatability issues in CE are caused by inconsistent velocities of the EOF. Unless the analyte undergoes a time-dependent change in its molecular charge-to-size ratio or the applied electric field strength is imprecisely controlled (both issues are rare), the  $\mu_{\text{ep}}$  of an analyte remains stable. In contrast, even under optimized conditions, the  $\mu_{\text{EOF}}$  fluctuates in response to changes in the ionic strength of the buffer and the conditioning of the capillary surface, as well as slight variations in pH and temperature.<sup>38</sup> In conventional CE experiments, when analyte mobilities are relatively high, small variations in EOF result in insignificant changes to  $\mu_{\text{tot}}$ ; however, when  $\mu_{\text{tot}}$  is small, the same variations in EOF will have a pronounced impact on the repeatability of analyte migration. Moreover, it is likely that the stability of EOF in PBS is worse than in CB. Electric current passing through an electrolyte solution causes ion depletion and formation of pH gradients, as consequences of electrophoresis and electrolysis, respectively. In CB-KCE, these changes occur on a much larger time scale than the time of analysis, ensuring that constant velocities are maintained throughout the experiment. Compared to CB, PBS consists of smaller, more mobile ions and has a lower buffering capacity, making it likely that considerable depletion of ions and establishment of pH gradients occur before analysis is complete. All of these instabilities will have a pronounced effect on  $\mu_{\text{EOF}}$ .

To assess and compare the stability of EOF in CB and PBS, we conducted an interval injection experiment, in which several injections of neutral marker were made at equal time intervals, and electrophoresis was performed without buffer replenishment between the injections. Any changes in the elution time of the neutral marker with consecutive injections indicate a change in  $\mu_{\text{EOF}}$  and signify the depletion of the buffer in the reservoirs. As expected, for CB the elution velocity of the neutral marker remained stable over the 20 min duration of the experiment (Figure 4). For PBS, however, within the first 8 min of electrophoresis, the velocity of EOF had decreased sufficiently to prevent marker detection. This confirmed our speculations about the susceptibility of PBS to fast ion depletion. Interestingly, no significant pH or conductivity changes were observed in the PBS buffer reservoirs after the 8 min of electrophoresis, suggesting that the decrease in  $\mu_{\text{EOF}}$  was predominantly caused by the change in nonproton ionic content of the buffer. Given the complicated and transient nature of capillary surface charge distribution in response to a changing ionic background, it is the most likely explanation for the poor repeatability of migration times in PBS-KCE.

The poor stability of EOF in PBS-NECEEM suggests that the above-measured estimate of DNA's  $\mu_{\text{tot}} = 0.003 \text{ mm}^2 \text{ V}^{-1}$

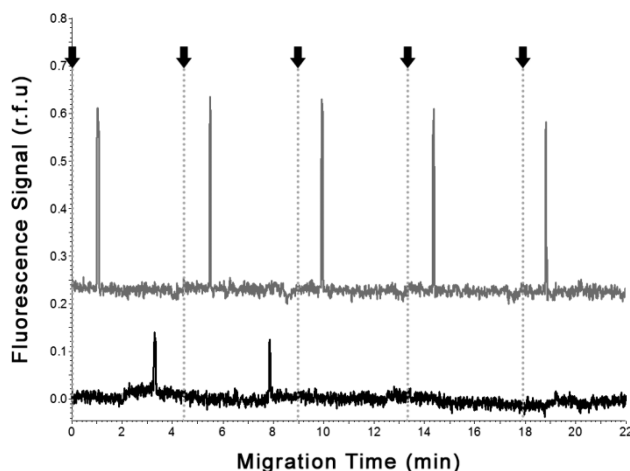


**Figure 4.** EOF stability test. A plug of 100 nM BODIPY was injected every 260 s, and electrophoresis was carried out between the injections from the same set of buffer reservoirs. Elution time of the neutral marker peak from the time of each injection (marked by the arrow and dotted vertical line) is indicative of the EOF velocity over the increasing time of electrophoresis. Experiment was performed with CB (top trace) and PBS (bottom trace) as run buffers. No signal was recorded during vial switching and between sample injection and electrophoresis steps.

$\text{min}^{-1}$  represents a time averaged value; i.e., its magnitude is larger in the beginning of the experiment and becomes smaller as buffer depletion continues. It may even be possible, if allowed enough time, that  $\mu_{\text{EOF}}$  decreases to a point that  $\mu_{\text{tot}}$  of DNA becomes negative, causing the DNA molecules to start migrating back toward the anode, never reaching the detector. As such, it is important to perform PBS-KCE experiments in less than 10 min, before the effects of buffer depletion set in.

**Peak Broadening.** Lastly, as observed in Figure 3, electrophoresis in PBS causes the width of the DNA peak to increase by approximately 10 times compared to peak widths in CB (after normalizing by residence time in the detector, Figure S3). Some of this peak broadening can be ascribed to the pressure propagation step, which was introduced to decrease the effective length of the capillary to 1.1 cm, as it increases peak widths by approximately 3 times (Figure S2). However, all of our NECEEM experiments incorporate a pressure propagation step to avoid the uncooled portion of the capillary, meaning that this level of broadening will be present in all our experiments. Additional peak broadening, however, can aggravate the issue of poor DNA detectability, if the local concentration of the analyte decreases below the limit of detection in significant parts of the sample zone.

In CE, peak smearing can occur either as a result of electro-dispersive phenomena (e.g., antistacking), sample interaction with the walls of the capillary, or due to interaction of the analyte with other species in the solution. Electro-dispersive peak smearing (antistacking) occurs when the ionic strength of the sample solution is significantly higher than that of the run buffer.<sup>39</sup> In our experiments, the sample buffer was always matched to the run buffer, eliminating the possibility of antistacking. Moreover, antistacking affects all analytes in the sample, while in our previous tests, no signs of dispersal for peaks of BODIPY or fluorescein were observed (Figure 2). The surface of a bare-silica capillary is negatively charged, akin to DNA, which makes the interactions between the sample and the walls unlikely. Nevertheless, to exclude the possibility of

ion-facilitated DNA–silica interactions, we have conducted a pressure propagation test for analyte adsorption onto capillary wall as described previously,<sup>40</sup> where a sample of DNA is driven through the capillary by pressure, with subsequent washes with NaOH and HCl. The harsh pH conditions disrupt electrostatic interactions between the sample and the walls and allow the adsorbed molecules to elute and be detected. Expectedly, during both the NaOH and HCl washes, no additional elution of DNA was observed, suggesting that no adsorption of DNA on the capillary walls occur (Figure S4).

In PBS-KCE experiments, DNA is always surrounded by a high concentration of  $\text{Na}^+$  and  $\text{K}^+$ , which can interact with its backbone and partially neutralize its charge. If these counterion–DNA complexes are stable over a comparable amount of time that it takes to spatially separate DNA molecules of various degree of neutralization (i.e., on the order of seconds or minutes), then dynamic peak broadening will ensue. In fact, the KCE technique of equilibrium capillary electrophoresis of equilibrium mixtures (ECEEM) relies on such peak broadening to measure the kinetics of molecular interactions.<sup>41</sup> We have recently reported that DNA can form stable complexes with metal counterions, including  $\text{Na}^+$  and  $\text{K}^+$ , which dissociate on a minute-time scale.<sup>42</sup> Such interactions, thus, are a feasible explanation for the observed peak broadening. To verify this hypothesis, we have performed electrophoresis in a 2-time dilution of PBS and observed approximately 3-time reduction in peak width when normalized by migration velocity (Figure S3). These observations strongly support the notion that DNA peak broadening in PBS-KCE occurs as a result of its interaction with the increased background of counterions. In this scenario, the longer the DNA sample is subjected to electrophoresis in the high ionic strength environment, the broader its peak becomes; thus, decreasing the duration of PBS-KCE experiments should help mediate this issue as well.

**Pressure-Facilitated KCE.** The phenomena described in the previous sections combine in a synergistic manner. The near-zero velocity of DNA causes the time of its migration to the detector to be excessively long, while buffer depletion and peak broadening are progressively aggravated with time. Thus, to alleviate the DNA detection issue in PBS-KCE, the analysis time must be significantly shortened. The most direct approach to achieve this is to reduce the physical length of the capillary; however, given the estimates of DNA mobility and ion-depletion time reported in previous sections, the capillary would have to be shortened to less than 1 cm, a feature difficult to implement. This can be somewhat offset by increasing the volume of the buffer reservoirs, to allow for slower buffer depletion. However, both of these changes require a high degree of customization to the CE instrument. Given the prevalence of commercial CE instrumentation, a convenient solution to the DNA detectability problem in PBS-KCE should rely on commonly available features and capabilities of such tools. An alternative approach to reducing CE analysis time, which is easily realized in most CE machines, involves supplementation of electrophoresis with a pressure-driven hydrodynamic flow. This essentially adds an additional velocity vector to all analytes, which offsets the drop in  $\mu_{\text{EOF}}$  in PBS, and brings  $\mu_{\text{tot}}$  of DNA to a more practical magnitude. Since pressure-driven velocity can be finely controlled, the total analysis time in PBS-KCE can be matched to that in CB-KCE, an added advantage for our comparative study.

When applying a hydrodynamic flow, we must keep in mind the shape of its profile, which unlike the flat-fronted EOF, is

parabolic. A significant flow velocity difference between the center and the boundaries of the capillary lumen cause deformation and asymmetry in resulting peaks, which makes signal area deconvolution more difficult in KCE.<sup>43</sup> This behavior, however, can be alleviated by using slow hydrodynamic flows or by using capillaries of a smaller inner diameter, where parabolicity of the flow profile is smoothed out by transverse diffusion. Before performing PBS-NECEEM analysis, we have confirmed that pressure-assisted KCE in PBS, performed in the same capillary setup as in the previously discussed CB-NECEEM experiment, does not cause significant peak aberrations (Figure S5). These experiments were also used to estimate analytical performance parameters of pressure-assisted KCE, namely, the precision of analyte migration time to detector, which had a relative error of 0.6%, and the reproducibility of peak area measurements for a given analyte, which had a relative error of less than 2.4%. Using the pressure-assisted KCE has, at last, allowed us to perform the PBS-NECEEM analysis which initiated this troubleshooting effort (Figure 1B). The  $K_d$  value measured with PBS-NECEEM was  $6.2 \pm 1.2$  nM, which is smaller than the CB-NECEEM results by nearly an order of magnitude. This suggests that the conformations of the aptamer and the protein are more favorable to form and maintain the complex in the high-ionic environment of PBS, in which the aptamer was selected. The  $K_d$  value obtained in the PBS-NECEEM experiment is also much closer to the results of the nitrocellulose binding assay reported upon the original characterization of the aptamer.<sup>30</sup> While the original publication reports the  $K_d$  as 0.096 nM, closer inspection of the data suggests that this value might have been underestimated. The value was obtained by fitting experimental data to a theoretical equation of a binding curve; however, the fairly large variance in replicates and abnormalities in the shape of the binding curve, which can be observed in the original figure (Figure 5C in ref 30), may have caused the fitting algorithm to return a value with a significant systematic error. Visual analysis of the published binding curve suggests that the half-binding point (which corresponds to  $K_d$  for 1:1 interactions) is reached at PDGF concentration of approximately 1 nM, which is a more conservative estimate of the  $K_d$  of this interaction. With this in mind, the value produced by our PBS-NECEEM is in line with the original characterization of the aptamer.

**Concluding Remarks.** The main cause of poor DNA detectability in PBS-KCE is the close match between time-averaged magnitudes of  $\mu_{\text{EOF}}$  and  $\mu_{\text{eph}}$  vectors of opposing signs, which combine into a near-zero value of DNA  $\mu_{\text{tot}}$ . When dealing with phenomena which are based on narrowly defined thresholds, it is important to question whether they result from a very specific set of employed conditions or whether they will manifest in a broad range of scenarios. In other words, it is important to understand whether other researchers are likely to experience similar problems and whether our described method of troubleshooting will be of a wide interest. The use of PBS as a KCE running buffer is warranted when emulating physiological conditions, a common provision in analysis of biomolecules. Depending on the model organism in question, such physiological conditions are defined quite narrowly in terms of temperature, pH, and ionic content. PBS, in particular, is universally formulated, with occasional supplementation with sub-mM concentrations of  $\text{MgCl}_2$  and  $\text{CaCl}_2$ , which will have a negligible effect on  $\mu_{\text{EOF}}$ . Theoretically,  $\mu_{\text{EOF}}$  depends on the zeta potential of the capillary wall (dependent on pH),



dielectric constant of the background electrolyte (dependent on ionic strength), and viscosity (dependent on temperature), all factors that will hold constant for all PBS-KCE experiments that use bare-silica capillaries. As for the  $\mu_{\text{eph}}$  of DNA, it remains unchanged across a wide range of molecular sizes,<sup>44–46</sup> as a result of the nearly constant mass-to-charge ratio of this polymer. The use of capillary coatings, especially those that stabilize EOF, might be an alternative method to overcome the described issues of poor DNA detectability; however, the use of the negatively charged bare-silica capillaries is preferential in analysis of DNA due to its simplicity and absence of DNA–capillary wall interactions. The use of capillary coatings which suppress EOF is not desired, as it will cause issues in analysis of positively charged DNA binders. Under suppressed EOF, negative DNA and any positively charged analytes will migrate in opposite directions, making it difficult to quantify both in the same run. Suppressed EOF will also lead to longer analysis times (due to slower analyte velocities), which will exacerbate the issue of PBS depletion. The use of coatings that reverse the EOF will decrease the separation efficiency between DNA and most proteins, large molecules which tend to comigrate with the EOF, making this option nonrobust. Due to better heat dissipation properties, experiments performed in capillaries of smaller inner diameters may employ higher electric field strengths to maintain the required in-capillary temperatures; however, such increases of the applied electric field strength would not exceed 2–5 times and, thus, would not be sufficient to decrease the DNA migration time to the detector to a practical level. It should be noted that applying a pressure flow (to decrease the analysis time), while at the same time decreasing the strength of the applied electric field (to account for the increased Joule heating), can significantly reduce the separation efficiency of CE. In our case, separation between DNA and the DNA–protein complex was still sufficient to accurately measure analyte peak areas; however, depending on the studied molecules, the experimenters must ensure that a sufficiently long capillary is used to allow for a better-than-baseline separation between the DNA and its complex. Taking a stock of all these considerations, it is likely that the majority of KCE experiments that aim at analysis of DNA–ligand interactions in PBS will experience the described issues. It is plausible that the insofar absence of PBS-KCE results for DNA is explained by the fact that some researchers have already encountered this problem in the past. We hope that, with the availability of the described here troubleshooting technique, the use of more appropriate physiological conditions will become more widespread in KCE analyses, which has the potential to improve the relevance and robustness of KCE methods at large.

## ■ ASSOCIATED CONTENT

### ■ Supporting Information

The Supporting Information is available free of charge on the ACS Publications website at DOI: 10.1021/acs.analchem.6b02117.

Nonrepeatability issues due to analyte interaction with sample vial; effects of pressure propagation on precision and accuracy of measurements of analyte mobility and peak broadening; dynamic DNA peak broadening in PBS-KCE; absence of DNA adsorption onto bare-silica capillary wall; effects of pressure-assisted electrophoresis on peak shape and width (PDF)

## ■ AUTHOR INFORMATION

### Corresponding Author

\*E-mail: skrylov@yorku.ca.

### Notes

The authors declare no competing financial interest.

## ■ ACKNOWLEDGMENTS

This work was funded by Natural Sciences and Engineering Research Council of Canada (Discovery grant 238990). M.K. was supported by an Alexander Graham Bell Canada Graduate Scholarship.

## ■ REFERENCES

- (1) Kaur, H.; Yung, L.-Y. L. *PLoS One* **2012**, *7*, e31196.
- (2) Chandrasekaran, A. R.; Pushpanathan, M.; Halvorsen, K. *Mater. Lett.* **2016**, *170*, 221–224.
- (3) Douglas, S. M.; Bachelet, I.; Church, G. M. *Science* **2012**, *335*, 831–834.
- (4) Krishnan, Y.; Simmel, F. C. *Angew. Chem., Int. Ed.* **2011**, *50*, 3124–3156.
- (5) Forster, R. E.; Hert, D. G.; Chiesl, T. N.; Fredlake, C. P.; Barron, A. E. *Electrophoresis* **2009**, *30*, 2014–2024.
- (6) Wheeler, D. A.; Srinivasan, M.; Egholm, M.; Shen, Y.; Chen, L.; McGuire, A.; He, W.; Chen, Y. J.; Makhijani, V.; Roth, G. T.; Gomes, X.; Tartaro, K.; Niazi, F.; Turcotte, C. L.; Irzyk, G. P.; Lupski, J. R.; Chinault, C.; Song, X. Z.; Liu, Y.; Yuan, Y.; Nazareth, L.; Qin, X.; Muzny, D. M.; Margulies, M.; Weinstock, G. M.; Gibbs, R. A.; Rothberg, J. M. *Nature* **2008**, *452*, 872–876.
- (7) Liu, Y. J.; Rauch, C. B.; Stevens, R. L.; Lenigk, R.; Yang, J. N.; Rhine, D. B.; Grodzinski, P. *Anal. Chem.* **2002**, *74*, 3063–3070.
- (8) Wegman, D. W.; Krylov, S. N. *Angew. Chem., Int. Ed.* **2011**, *50*, 10335–10339.
- (9) Becker, C.; Hammerle-Fickinger, A.; Riedmaier, I.; Pfaffl, M. W. *Methods* **2010**, *50*, 237–243.
- (10) Berezovski, M.; Krylov, S. N. *Anal. Chem.* **2005**, *77*, 1526–1529.
- (11) Galievsky, V. A.; Stasheuski, A. S.; Krylov, S. N. *Anal. Chem.* **2015**, *87*, 157–171.
- (12) Mosing, R. K.; Mendonsa, S. D.; Bowser, M. T. *Anal. Chem.* **2005**, *77*, 6107–6112.
- (13) Petrov, A.; Okhonin, V.; Berezovski, M.; Krylov, S. N. *J. Am. Chem. Soc.* **2005**, *127*, 17104–17110.
- (14) Lou, B. L.; Chen, E.; Zhao, X. Y.; Qu, F.; Yan, J. Y. *J. Chromatogr. A* **2016**, *1437*, 203–209.
- (15) Kanoatov, M.; Galievsky, V. A.; Krylova, S. M.; Cherney, L. T.; Jankowski, H. K.; Krylov, S. N. *Anal. Chem.* **2015**, *87*, 3099–3106.
- (16) Riley, K. R.; Gagliano, J.; Xiao, J. J.; Libby, K.; Saito, S.; Yu, G.; Cubicciotti, R.; Macosko, J.; Colyer, C. L.; Guthold, M.; Bonin, K. *Anal. Bioanal. Chem.* **2015**, *407*, 1527–1532.
- (17) Mironov, G. G.; Okhonin, V.; Khan, N.; Clouthier, C. M.; Berezovski, M. V. *ChemistryOpen* **2014**, *3*, 58–64.
- (18) Ashley, J.; Li, S. F. Y. *Anal. Biochem.* **2013**, *434*, 146–152.
- (19) Ashley, J.; Ji, K. L.; Li, S. F. Y. *Electrophoresis* **2012**, *33*, 2783–2789.
- (20) Clouthier, C. M.; Mironov, G. G.; Okhonin, V.; Berezovski, M. V.; Keillor, J. W. *Angew. Chem., Int. Ed.* **2012**, *51*, 12464–12468.
- (21) Carrasco-Correa, E. J.; Beneito-Cambra, M.; Herrero-Martinez, J. M.; Ramis-Ramos, G. J. *Chromatogr. A* **2011**, *1218*, 2334–2341.
- (22) Yang, P.; Mao, Y.; Lee, A. W. M.; Kennedy, R. T. *Electrophoresis* **2009**, *30*, 457–464.
- (23) Sloat, A. L.; Roper, M. G.; Lin, X. L.; Ferrance, J. P.; Landers, J. P.; Colyer, C. L. *Electrophoresis* **2008**, *29*, 3446–3455.
- (24) Li, T.; Wang, H. L. *Anal. Chem.* **2009**, *81*, 1988–1995.
- (25) Keefe, A. D.; Pai, S.; Ellington, A. *Nat. Rev. Drug Discovery* **2010**, *9*, 537–550.
- (26) Xu, C.-X.; Yin, X.-F. *J. Chromatogr. A* **2011**, *1218*, 726–732.
- (27) Li, S. K.; Liddell, M. R.; Wen, H. J. *Pharm. Biomed. Anal.* **2011**, *55*, 603–607.

- (28) Jia, Z. J.; Ramstad, T.; Zhong, M. J. *Pharm. Biomed. Anal.* **2002**, 30, 405–413.
- (29) Ichiki, T.; Ujiie, T.; Shinbashi, S.; Okuda, T.; Horiike, Y. *Electrophoresis* **2002**, 23, 2029–2034.
- (30) Green, L.; Jellinek, D.; Jenison, R.; Ostman, A.; Heldin, C.; Janjic, N. *Biochemistry* **1996**, 35, 14413–14424.
- (31) Musheev, M. U.; Filiptsev, Y.; Krylov, S. N. *Anal. Chem.* **2010**, 82, 8692–8695.
- (32) Patel, K. H.; Evenhuis, C. J.; Cherney, L. T.; Krylov, S. N. *Electrophoresis* **2012**, 33, 1079–1085.
- (33) Evenhuis, C. J.; Musheev, M. U.; Krylov, S. N. *Anal. Chem.* **2011**, 83, 1808–1814.
- (34) Lakowicz, J. R., Ed. *Principles of Fluorescence Spectroscopy*; Springer US: Boston, MA, 2006; pp 205–235.
- (35) Kanoatov, M.; Krylov, S. N. *Anal. Chem.* **2011**, 83, 8041–8045.
- (36) Chang, C. H.; Wang, Y.; Gupta, P.; Goldenberg, D. M. *mAbs* **2015**, 7, 199–211.
- (37) Panchuk-Voloshina, N.; Haugland, R. P.; Bishop-Stewart, J.; Bhargat, M. K.; Millard, P. J.; Mao, F.; Leung, W. Y.; Haugland, R. P. *J. Histochem. Cytochem.* **1999**, 47, 1179–1188.
- (38) Lim, C. Y.; Lim, A. E.; Lam, Y. C. *Sci. Rep.* **2016**, 6, 22329.
- (39) Meurant, G. *Practical Capillary Electrophoresis*; Elsevier Science: Atlanta, GA, 2012; pp 269–273.
- (40) de Jong, S.; Krylov, S. N. *Anal. Chem.* **2012**, 84, 453–458.
- (41) Kanoatov, M.; Cherney, L. T.; Krylov, S. N. *Anal. Chem.* **2014**, 86, 1298–1305.
- (42) Musheev, M. U.; Kanoatov, M.; Krylov, S. N. *J. Am. Chem. Soc.* **2013**, 135, 8041–8046.
- (43) Kanoatov, M.; Retif, C.; Cherney, L. T.; Krylov, S. N. *Anal. Chem.* **2012**, 84, 149–154.
- (44) Viovy, J. L. *Rev. Mod. Phys.* **2000**, 72, 813–872.
- (45) Mayer, P.; Slater, G. W.; Drouin, G. *Anal. Chem.* **1994**, 66, 1777–1780.
- (46) Olivera, B. M.; Baine, P.; Davidson, N. *Biopolymers* **1964**, 2, 245–257.